http://doi.org/10.35784/iapgos.7643 received: 26.04.2025 | revised: 15.01.2026 | accepted: 02.06.2026 | available online: 30.06.2026

STROKE DETECTION FROM BRAIN CT-IMAGES AND ITS VOLUME VISUALIZATION

Rithu James[1], Appukuttan Harsha[1], Liza Annie Joseph[2]
[1]Rajagiri School of Engineering and Technology, Department of Electronics and Communication Engineering, Kochi, India, [2]Rajagiri School of Engineering and Technology, Department of Applied Electronics and Instrumentation Engineering, Kochi, India

Abstract. *This study presents a comprehensive methodology for the detection, classification, and volumetric analysis of stroke lesions from computed tomography (CT) images. The approach encompasses several key stages: Skull stripping is performed to remove non-brain tissues, enhancing the accuracy of subsequent analyses. Stroke regions are identified by analysing the symmetry between the two hemispheres of the brain in CT images. Advanced segmentation algorithms are applied to delineate the region of interest (ROI) corresponding to the stroke-affected area. Texture features from the segmented ROI are extracted to capture the characteristics of the stroke lesion. The extracted features are input into classifiers such as Support Vector Machines (SVM) and K-Nearest Neighbors (K-NN) to categorize the type of stroke. For haemorrhagic strokes, the segmented regions from the CT image stacks are used to visualize and quantify the volume of the stroke. The methodology was validated using datasets from five patients, demonstrating its potential in aiding clinical diagnosis and treatment planning for stroke patients.*

Keywords: computed tomography, stroke, feature extraction, voxels

WYKRYWANIE UDARU NA PODSTAWIE OBRAZÓW TK MÓZGU I WIZUALIZACJA JEGO OBJĘTOŚCI

Streszczenie. *W niniejszym badaniu przedstawiono kompleksową metodologię wykrywania, klasyfikacji i analizy objętościowej zmian udarowych przy użyciu obrazów tomografii komputerowej (TK). Podejście obejmuje kilka kluczowych etapów: wykonuje się stripping czaszki w celu usunięcia tkanek innych niż mózg, co zwiększa dokładność kolejnych analiz. Obszary udaru są identyfikowane poprzez analizę symetrii między dwiema półkulami mózgu na obrazach TK. Zaawansowane algorytmy segmentacji są stosowane w celu określenia obszaru zainteresowania (ROI) odpowiadającego obszarowi dotkniętemu udarem. Cechy tekstury z segmentowanego ROI są ekstrahowane w celu uchwycenia cech zmiany udarowej. Wyekstrahowane cechy są wprowadzane do klasyfikatorów, takich jak Support Vector Machines (SVM) i K-Nearest Neighbors (K-NN), aby sklasyfikować rodzaj udaru. W przypadku udarów krwotocznych segmentowane obszary ze stosów obrazów TK są wykorzystywane do wizualizacji i ilościowego określenia objętości udaru. Metodę tę potwierdzono zbiorami danych pochodzącymi od pięciu pacjentów, wykazując jej potencjał we wspomaganiu diagnostyki klinicznej i planowania leczenia pacjentów po udarze.*

Słowa kluczowe: tomografia komputerowa, udar, ekstrakcja cech, woksele

Introduction

Stroke occurs when there is a poor blood supply to the brain, either due to bleeding or blood blockage inside the brain. Recent global studies have highlighted a significant rise in stroke incidence and mortality, positioning stroke as a leading contributor to neurological health burdens worldwide. With the increase in global life expectancy, the prevalence of age-related conditions like stroke rises correspondingly. Ischemic strokes, which account for about 87% of all strokes, are caused by a blockage of the blood supply, while haemorrhagic strokes, accounting for around 13%, are caused by bleeding in the brain. Haemorrhagic strokes are generally more fatal than Ischemic strokes. In both ischemic and haemorrhagic strokes, stroke volume refers to the amount of brain tissue affected by the stroke.

Computed tomography (CT) scan is preferred over the MRI (Magnetic resonance imaging) for brain imaging due to its wider availability, lower cost and sensitivity to early stroke. Unenhanced CT, a 16-bit DICOM (Digital Imaging and Communication in Medicine) grayscale image, can help identify early signs of stroke and can help rule out haemorrhage [3].

CT makes use of X-rays to create cross-sectional, two-dimensional images of the body. Each obtained CT slice is divided into a matrix of 1024×1024 volume elements. Each voxel has been traversed by X-ray photons during the scan and the detector measures the intensity of the radiation transmitted. The density or the attenuation values of the tissue at each point in the slice is calculated using the intensity values. Each pixel has a specified attenuation value. The image viewed is obtained as the reconstruction of a matrix of pixels. Each pixel is assigned a numerical value called CT number and it is the mean of all the attenuation values contained within the corresponding voxel.

CT has the ability to quantify the beam absorption capability of an object. The CT number is expressed using Hounsfield units (HU) named after Sir Godfrey Hounsfield. It is acquired by the linear transformation of the attenuation coefficients measured. The dynamic range of HU is from -1000 HU to +1000 HU. Hounsfield assigns 0 for water and -1000 for air and +1000 for bone. Medical scanners typically work in a range of -1024 HU to +3071 HU. The objects having attenuation capacity less than that of water has negative CT numbers and those having greater attenuation capacity have positive CT numbers. The degree of absorption of X-rays is proportional to the density values of the tissue. If the density is more, attenuation will be high and greater will be the CT number [8]. The range of attenuation coefficients of the material determines its CT values [2, 20].

The mean grey level value range in HU for ischemic and haemorrhagic stroke is ~10-20 HU and 50-80 HU, respectively. In brain CT images, Ischemic stroke appears as darker regions, whereas Haemorrhagic stroke appears as brighter regions, as shown in Figure 1a and 1b.

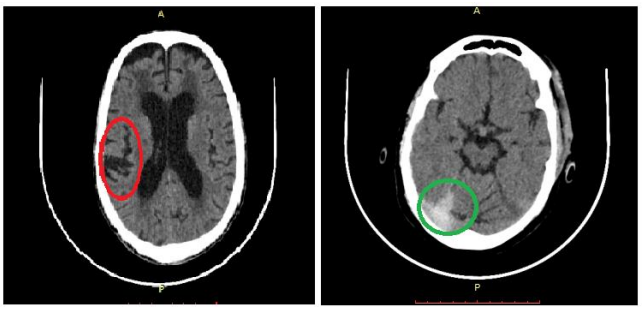

a) *b)*

Fig. 1. CT image of (a) ischemic, b) haemorrhagic stroke

The authors in [9] devised a method to find stroke from CT images. The cohesive rate of pixels of CT images is calculated to find the probability of stroke. A method to classify abnormal CT images into acute, haemorrhage and chronic infarct is devised in [4]. This method uses midline symmetry detection and analysis. Intensity-based and transforms are used to detect the abnormality and the main advantage of this method is its ability to detect and segment all types of stroke.

The method for classifying abnormal CT images [14] involves three main steps: image enhancement, midline symmetry detection, and analysis. The line of symmetry is identified such that the horizontal line through the centre of the slice is intersected by the symmetry line passing through the tip of the nose.

The paper [1] aims to develop an intelligent and accurate system for doctors and radiologists to diagnose haemorrhage and specify the type of haemorrhage using Fuzzy C-means and watershed algorithm and using neural networks for the classification of haemorrhage. Its implementation has pre-processing, segmentation, feature extraction and classification [5]. The pre-processing is done by thresholding and morphological operations to remove the skull. Region growing is used for segmentation [15]. Features like size of region-of-interest (ROI), centroid, perimeter, etc are extracted and these features are fed to the classifier for the classification.

Early signs of haemorrhagic stroke [27], which further delayed can lead to the chronic stage or even death. The study [17] proposed hybrid algorithms incorporating a novel convolutional neural network (CNN) architecture named OzNet, along with various machine learning techniques, for the binary classification of real brain stroke CT images. Recent individual deep learning studies have applied vision transformer (ViT)-based architectures and hybrid models to classify stroke types on CT scans with high overall accuracy (e.g., ~98% accuracy and F1-score), often integrating explainable AI techniques to improve clinical interpretability [22].

Traditionally, medical imaging systems used 2D visualization of human organs whereas latest study has brought many advancements in digital medical imaging systems and is able to create both 2D as well as in, some cases 3D images of human organs [18]. The surface rendering and volume visualization are regularly used in 3D modelling of 2D medical images from CT or MRI, which helps in decision on the treatment planning.

Pre-processing stage of the original CT scan image includes image enhancement and noise filtering, skull stripping. Then the stroke area is segmented using the active contour model without edges. With the segmented stroke area, features like Tamura features, GLCM features and statistical features are extracted. The extracted features are subsequently input into the classifier to distinguish between ischemic and haemorrhagic strokes. Support Vector Machine (SVM) and K-Nearest Neighbour (K-NN) classifiers are employed for this purpose. The performance of the classifiers is evaluated using specificity, sensitivity, and accuracy metrics. The segmented part of haemorrhagic stroke from the original Brain CT-scan is used for volume visualization using Marching Cube (MC) algorithm.

1. Segmentation and classification

The work is carried out on data set of 5 patients from a hospital with all scan parameters and annotations/ground truth description files. Each patient's database has 200–600 images of size 512×512 with a bit depth of 12. A CT image before and after window setting at a window centre of 40HU and width of 80 HU CT images are inherently 16-bit in size. A DICOM (16-bit) to grey (8-bit) conversion is used, which sets up a window between values 0 to 80 HU, the range of values containing the required information. The values below 0 HU are converted to 8-bit 0 value and those above 80 HU are converted to 255. The haemorrhage will be mapped to a 8-bit value range between 200 and 255.

Each CT scan consists of multiple slices, typically exceeding 300 per patient. However, not all slices contain diagnostically relevant information for stroke classification. Therefore, a subset of slices was selected based on the presence of visible stroke regions, resulting in a total of 800 images across five patients.

To avoid redundancy and ensure meaningful learning, slices without pathological findings were excluded. The selection process focused on representative slices capturing ischemic and haemorrhagic regions.

The resultant image after windowing is K-means clustered [24]. The required cluster is selected and segmented out. Thresholding and watershed algorithm is applied to the converted 8-bit image. The Otsu's thresholding [16] is used to segment out the stroke and the bone region is removed. Then distance transform is applied and the watershed function is applied to the distance transform matrix to get the different regions of intensities of stroke. In the region growing algorithm, an initial seed point was selected and the required region was iteratively grown by comparing the seed region with the neighbouring pixels [6].

1.1. Preprocessing

Skull stripping is an important step to remove the non-cerebral tissue, which are not regions of interest in this study. In this work, skull stripping is done using morphological operations and thresholding. The image then underwent a series of operations like Otsu thresholding, dilation and erosion for skull stripping [26].

The original enhanced Ischemic stroke and Haemorrhagic stroke images are shown in Figure 2a and Figure 3a. The skull stripped images are shown in Figure 2b and Figure 3b.

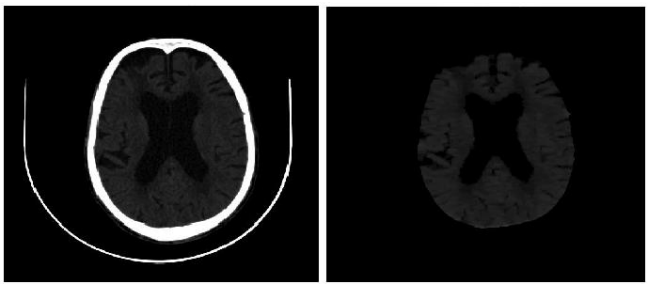

a) *b)*

Fig. 2. a) Enhanced ischemic stroke image, b) preprocessed image

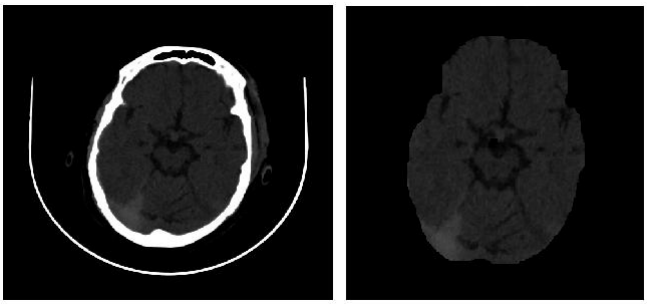

a) *b)*

Fig. 3. a) Enhanced haemorrhagic stroke image, b) preprocessed image

After the skull stripping, the image is divided into two halves using the line of symmetry as shown in Figure 4a. Each half is again divided into 32×32 patches as in Figure 4b.

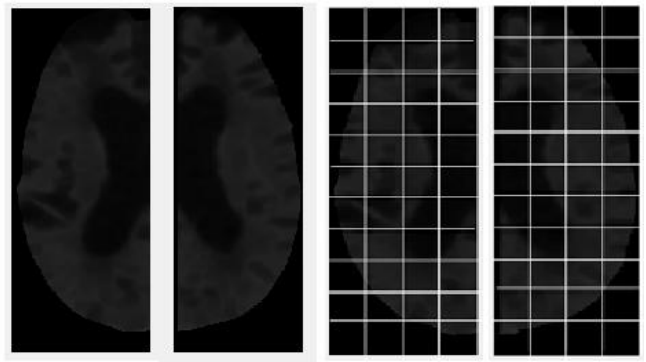

a) *b)*

Fig. 4. a) Two halves of the image, b) halves divided into patches

Histogram of each half is taken and if there is a difference in the histograms of the two halves, correlation between the two patches are calculated.

If the correlation is below a threshold value, there exists some abnormality in the image. For the ischemic stroke image, taken correlation threshold value is set as 0.5. To identify which half the abnormality is present, wavelet decomposition is done to obtain the energy. If the energy of one half is greater than the other, the one with maximum energy is taken, which has the abnormality.

1.2. Segmentation

The Otsu's thresholding method is used to segment out the stroke and the bone region is removed. In the Otsu's method, each possible value for threshold value is taken and then the features of the class that lies above it and below it is analysed. Then a value is selected which minimises the within-class variances. Figure 5 shows the segmented region in haemorrhagic and ischemic stroke images.

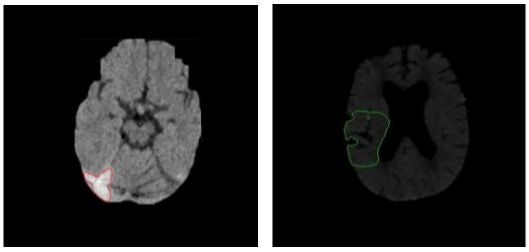

Fig. 5. Segmented region in haemorrhagic and ischemic stroke images

1.3. Feature extraction

The Haralick features are a set of 13–28 statistical measures derived from the grey-level co-occurrence matrix (GLCM) that capture various aspects of textures for the Ischemic stroke image are shown in Figure 6.

Tamura texture features depend on the human visual system. There exist six textural features such as coarseness, contrast, directionality, line-likeness, regularity and roughness [19]. Wavelet transform helps in texture analysis and classification by making use of multi-resolution approach. It provides the information about the time-frequency representation [7]. Statistical features depend upon the statistical distribution of pixels, texture features are extracted. The statistical features are grouped into two: first-order and second-order statistics [21]. The first order statistics are the mean and the second order statistics include contrast, correlation, energy and entropy.

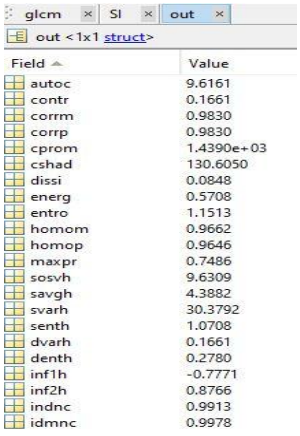

Fig. 6. Haralick features for the ischemic stroke

The choice of Haralick and Tamura features was motivated by their complementary ability to capture both statistical and perceptual texture characteristics in CT images. Haralick features effectively describe spatial grey-level dependencies, which are essential for identifying the homogeneous hypo-dense regions of ischemic stroke and the heterogeneous hyper-dense regions of haemorrhagic stroke. Tamura features, on the other hand, model perceptual texture properties such as coarseness and contrast, enhancing the representation of visually distinguishable patterns.

Table 1 shows the Tamura features and Table 2, the statistical features of Ischemic stroke and Table 3 shows the statistical features of haemorrhagic stroke.

Table 1. Tamura features ischemic stroke

Features	Ischemic Stroke	Normal
Coarseness	7.614435	12.0075462
Contrast	3.09104	3.2709652
Directionality	8.0156	9.33E-09

Table 2. Statistical features ischemic stroke

Features	Ischemic Stroke	Normal
Correlation	0.8652717	0.6488
Contrast	0.0137392	0.0085
Entropy	0.2563689	0.2555
Energy	0.8938166	0.8872

Table 3. Statistical features haemorrhagic stroke

Features	Normal	Haemorrhagic Stroke
Contrast	0.0595	0.1268
Correlation	466.0144	223.8289
Homogenity	0.606	0.8265
Energy	593.0633	645.3628
Entropy	0.314	0.4852
Moment	64.8418	60.1005

1.4. Classification

Features extracted from the segmented region are utilized for classification. The combination of Haralick and Tamura features provides a more comprehensive texture representation by integrating statistical and perceptual characteristics, improving discriminative power for stroke classification. The dataset was divided into training and testing sets using an 80:20 split at the patient level to ensure independence between the two sets. Images from the same patient were not shared across training and testing datasets. All preprocessing steps, including feature extraction and normalization, were performed independently within each data and subsequently applied to the test set. This prevented any information from the test data influencing the training process.

In this step, strokes are categorized into two types: ischemic and haemorrhagic. Classification is performed using a Support Vector Machine (SVM) [25], trained on a selected set of features. As a supervised learning algorithm, SVM seeks to determine a hyperplane that maximally separates the two classes. K-Nearest Neighbour (KNN) algorithm [10, 11] is a productive machine learning algorithm for effective classification as well as regression. The performance of the classifier, such as sensitivity, specificity and accuracy, depends on the error rate, which is represented in terms of true positive (TP), true negative (TN), false positive (FP) and false negative (FN).

Set up the training data - one set consisting of normal CT brain images and the other of stroke affected images. Features are extracted from all the images. Train the SVM by giving multiple images belonging to the 2 sets and the outputs are learned by the SVM model. Test the SVM model. The extracted features of the segmented region are fed to the SVM classifier for the classification of stroke-affected or normal.

The proposed model achieved a sensitivity of 77.7%, specificity of 88.89%, and accuracy of 83.33% with a 95% confidence interval (CI) of 65.53%–89.86%, 79.71%–98.07% and 72.45%–94.20%, respectively, indicating a moderate to high ability to correctly identify positive cases. The relatively wide interval reflects statistical uncertainty due to the small sample size and emphasizes the need for validation on larger datasets. The performance of the classifier is tabulated in Table 4.

Table 4. SVM performance ischemic stroke

N=90	Predicted Yes	Predicted No
Actual Yes	TP=35	FN=10
Actual No	FP=5	TN=40
Sensitivity=77.7%	CI=65.54%-89.86%	
Specificity=88.89%	CI=79.71%-98.07%	
Accuracy=83.33%	CI=72.45%-94.20%	

1.5. Performance evaluation of SVM and K-NN

The performance comparison between the classifiers is done by computing the accuracy, specificity and sensitivity of the classifier for Haemorrhagic stroke. Table 5 shows the performance comparison.

Table 5. Performance of SVM and K-NN

	Accuracy (%)		Specificity (%)		Sensitivity (%)		Build time (seconds)	
DATA	SVM	KNN	SVM	KNN	SVM	KNN	SVM	KNN
100	73.45	71.02	69.42	70.61	75.45	71.26	0.65	2.47
200	75.41	72.56	73.02	71.54	78.41	77.22	1.35	2.87
300	80.5	77.58	77.49	74.35	83.51	80.29	1.6	3.12
400	83.41	79.81	78.97	78.39	85.79	82.75	2.01	3.61
500	85.76	83.15	84.46	81.12	86.24	84.05	2.33	3.86
600	87.2	85.79	86.19	86.78	88.25	85.75	2.85	4.32

The accuracy, specificity and sensitivity of SVM are always higher compared to those of K-NN. As size of the training dataset increases, the accuracy of both classifiers increases. The build time is comparatively high for K-NN in most of cases. The selected feature sets and classifier configuration are supported by prior studies in medical image analysis.

2. Volume visualization

The segmented area is subjected to volume visualization using marching cube (MC) algorithm [25].

2.1. Marching cube algorithm

The segmentation output serves as the input for the MC algorithm to produce precise isosurfaces and 3D models. CT image is made up of small square matrix images of size 256×256 to 1024×1024. These pixels are in 2D. Since, a CT slice has a finite thickness along with other features, each pixel actually represents a small volume element, called a voxel in 3D space. During processing, multiple image slices are organized into a multidimensional array, with two adjacent slices considered at a time [13]. This is done for 5 patients; each dataset has around 50 slices, so in total, around 250 slices with haemorrhagic stroke are analysed.

A method for the automatic detection of haemorrhagic stroke and its volume in voxels is proposed. As per bleeding inside the brain, haemorrhagic stroke can be of two types: Subdural hematoma (SDH), a condition that may become chronic when shrinkage of the brain allows the brain to move more freely within the skull. Subarachnoid haemorrhage (SAH) results in the bleeding between the brain and the tissue covering the brain. Figure 7 and Figure 8 show the segmented regions of SDH and SAH haemorrhagic stroke, respectively. Figure 9 shows the SAH image after 5 iterations.

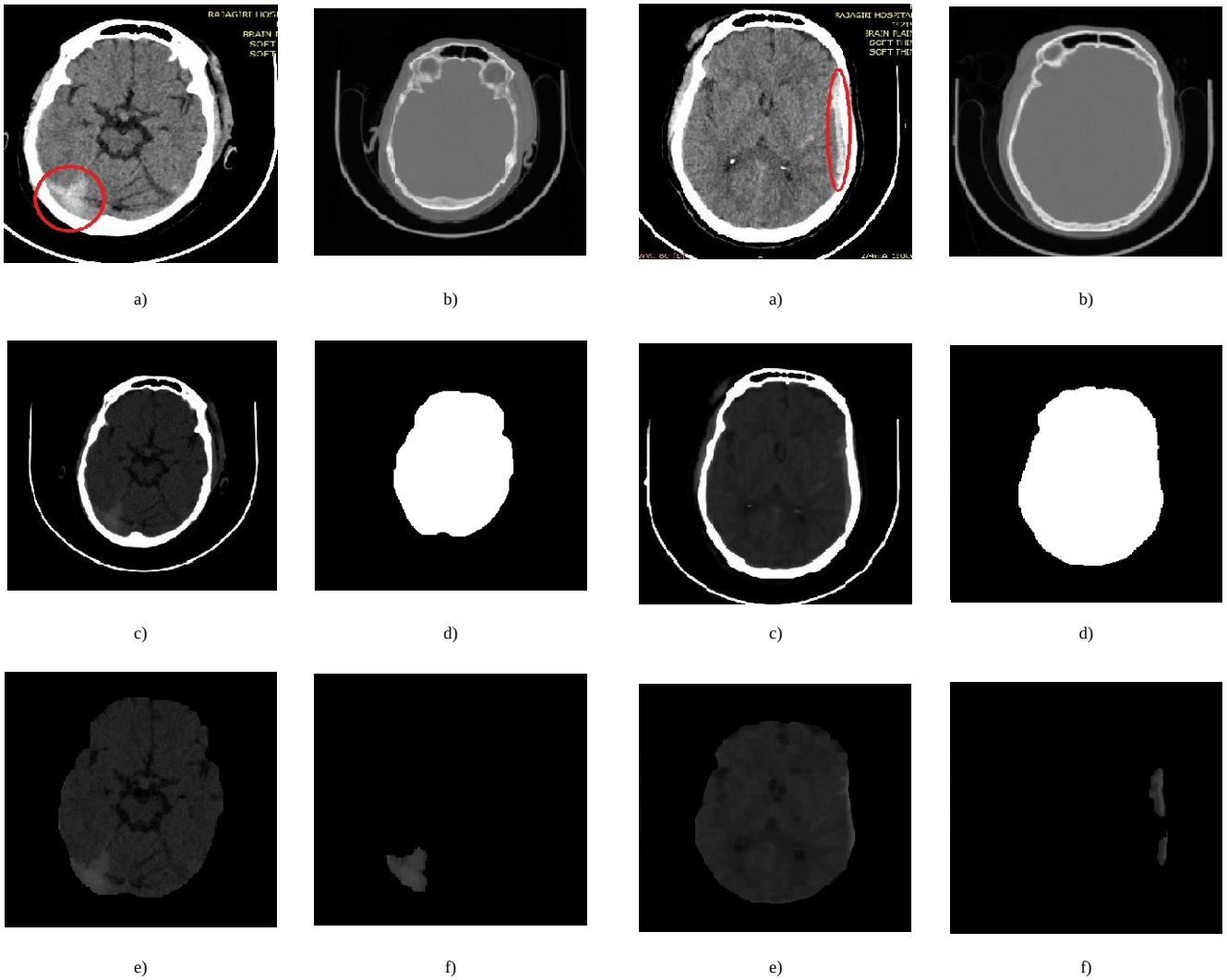

a) b) c) d) e) f)

Fig. 7. a) Subdural hematoma (SDH), b) image before enhancement, c) image after enhancement, d) image mask, e) processed image, f) segmented area

a) b) c) d) e) f)

Fig. 8. a) Subarachnoid haemorrhage (SAH), b) image before enhancement, c) image after enhancement, d) image mask, e) processed image, f) segmented area

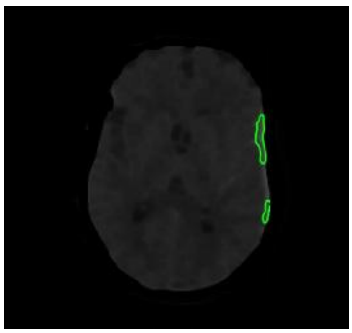

Fig. 9. Image after 5 iterations

2.2. Stacking and 3D modelling

The area of stroke is detected using HU information and then segmented using region-based active contour segmentation. The MC algorithm is applied on the segmented region for 3D modelling, and hence, the volume of the segmented area is calculated in voxels.

The segmentation is done for all the slices of the patient. These segmented images are then stacked and stored in an array. This stack is given to the MC algorithm to form the 3D model. For 3D modelling, the proposed algorithm is marching cube. First the mesh grid, a voxel in which the image has to reside is created (same size as the image). Iso value = 4, 8, 16, ...etc. As this value improves the shape of the image becomes much smoother. Here, the iso value is set to 8. Rotate the 3D model to view the region under different azimuth and elevation angles. The segmented image of the 30 slices is shown in Figure 10. The 3D model at different angles is shown in Figure 11.

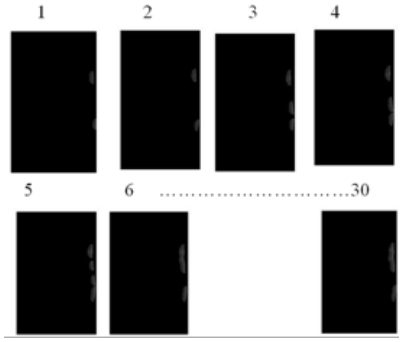

Fig. 10. The segmented image for 30 slices

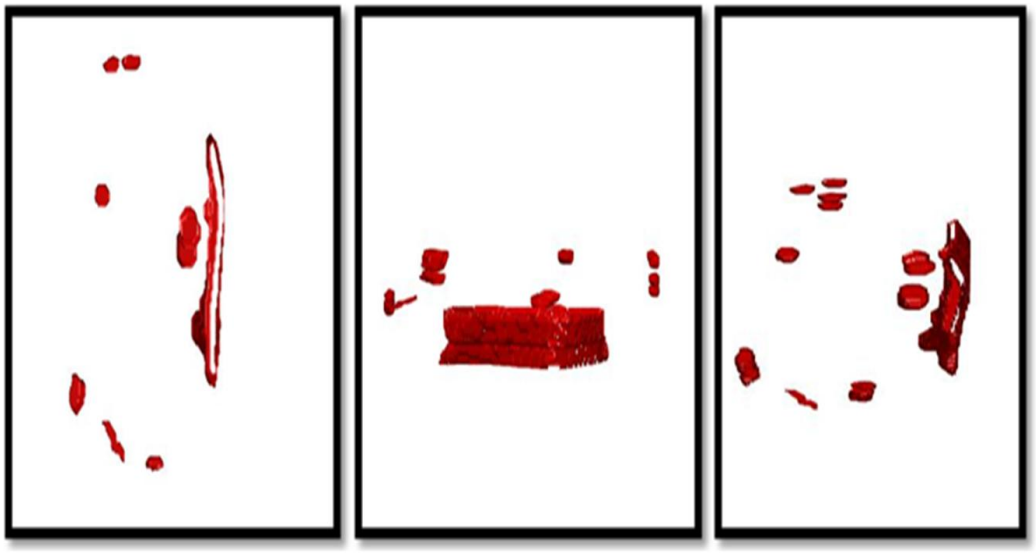

a) b) c)

Fig. 11. 3D model of haemorrhagic stroke and at different angles. a) Az: 0; EL: 90, b) Az: 90; EL: 12, c) Az: 1; EL: 21

2.3. Volume calculation

From the 3D model the largest area is considered as the region of stroke and rest of the areas are taken as false positives. These areas have to be eliminated from each slice. For the required area selection largest blob is to be identified. The most common method for blob detection is convolution. Once the largest blob is detected, its area is found for each slice. The volume is calculated as the product of the segmented area from each slice and the number of slices. Table 6 is giving an account of each patients affected slices and their volume in voxels.

Table 6. Volume of stroke affected area in voxel

Patient	No: of Slices	Volume of Segmented Area
A	15	6989
B	15	3516
C	38	13198
D	19	15879
E	30	41602

The volume of a 3D area is represented in voxels, as the area is multiplied by its thickness. When comparing patients C and E, patient C has more slices, but patient E has the highest volume; that is, the number of slices and volume are not in proportion. It entirely depends on the largest pixel area from each slice. As the volume increases, the depth of the stroke in voxels also increases. Patient E is affected by a stroke at 41602 voxel depth. If the pixel spacing is 0.45×0.45 mm and the slice thickness is 5 mm, then the voxel volume is 0.45×0.45×5 (1.0125 mm^3). Therefore total volume for pixel is 41602×1.0125 (42,122.025 mm^3) or 42.12 ml.

3. Result and discussion

Compared to the existing stroke detection and volume estimation techniques, the detection and volume estimation remains jointly optimized in the proposed methodology. The accurate detection and classification of stroke is very important for the treatment. The stroke area is segmented and then its textural features are taken for the classification. In the K-means clustering algorithm, low number of clusters could cause difficulty in segmenting the stroke region. This could be solved by increasing the number of clusters that need to be selected by the user, but it could be tiresome. In the thresholding and watershed algorithm, since the stroke could be in different slices of the brain for different patients, there may be changes in the threshold values which could affect segmentation

efficiency. In the region growing algorithm, due to the large number of pixels in the DICOM images, the number of iterations becomes too large and there is a significant time delay between the input and the output.

To avoid redundancy and ensure meaningful learning, slices without pathological findings were excluded. The selection process focused on representative slices capturing ischemic and haemorrhagic regions.

Classifiers such as SVM and K-NN methods can serve as efficient, interpretable baselines—particularly in resource-constrained settings There will be more than 300 slices per patient and each slice is considered an image. Out of 800 images, 75% are used to train the model, while remaining 25% are used to test how well the model is performing. SVM performs much better with 87.20% of accuracy, 88.25% of sensitivity, and 86.78% of specificity compared to K-NN classifier performance.

Importantly, to prevent data leakage and bias, the dataset was partitioned at the patient level. All slices from a given patient were included exclusively in either the training or testing set, ensuring that no overlap occurred between the two sets. This approach avoids overestimation of model performance due to intra-patient similarity.

The segmentation is done for 5 patients; each dataset has around 50 slices so in total around 250 slices with haemorrhagic stroke is analysed. These slices are then given to the standard 3D modelling techniques. Using MC algorithm, visualizations can be generated with relative ease. The use of 3D modelling to the segmented image helps doctors view brain stroke from different angles, find the depth, thickness, and location of stroke.

Compared with SVM and K-NN, deep learning approaches performance gains come with higher computational cost, and larger data requirements. In this work, SVM and K-NN were selected to provide a baseline comparison and to emphasize interpretability and computational efficiency with the available data set. Most deep learning models require substantially larger datasets for stable generalization. With limited data, such models are prone to overfitting unless extensive augmentation, transfer learning, or pretraining is applied. Moreover, CNNs and Vision Transformers involve a large number of learnable parameters, which increases the risk of overfitting in small datasets. Therefore, the proposed method may offer practical advantages in small-sample scenarios, though broader validation is still required. The relatively wide confidence interval, due to small data set appears good at detecting positives, but the estimate is not very precise. However, validation on a larger and more diverse dataset is required before clinical applicability can be established.

4. Limitations

The experimental validation is conducted on data from only five patients, which is insufficient to draw strong or clinically reliable conclusions. The use of five patients is considered acceptable for a proof-of-concept study for several reasons. Even though only five patients' data is used, for the segmentation and classification, the number of slices per patient vary from 200 to 600. The goal of this work is not to benchmark against state-of-the-art deep learning systems, but rather to evaluate the feasibility of classical machine-learning classifiers (SVM and K-NN) combined with handcrafted features for stroke detection. Volumetric medical imaging produces many voxels/slices per patient, allowing algorithmic behaviour to be analysed across diverse lesion appearances within each case.

Consequently, the results presented in this work should be interpreted as preliminary and exploratory, intended to demonstrate the technical feasibility of the proposed pipeline rather than to establish clinical effectiveness. Larger, multi-centre datasets will be required to validate robustness, generalizability, and clinical utility.

5. Conclusion and future scope

Despite the limited dataset size, the study provides valuable insights into the discriminative capability of combined texture features for distinguishing ischemic and haemorrhagic stroke. Future work will focus on validating the proposed approach on larger and more diverse datasets to improve robustness and clinical applicability.

The method can help pinpoint stroke locations accurately, aiding in diagnosis and treatment planning. By improving grey and white matter differentiation, early stroke detection and even detection of simultaneous strokes in both brain hemispheres could be achieved. 3D visualization further enhances diagnosis and treatment effectiveness. Future work will explore deep learning–based methods such as 3D CNNs/U-Net [23] variants to potentially improve performance further.

Conflict of interest

The authors declare no conflict of interest.

References

[1] Al-Ayyoub, M., Alawad, D., Al-Darabsah, K., & Aljarrah, I. (2013). Automatic Detection and Classification of Brain Hemorrhages. *WSEAS Transactions on Computers*, *12*(10), 395–405.

[2] Al-Janabi, O. M., El Refaei, A., Elgazzar, T., Mahmood, Y. M., Bakir, D., Gajjar, A., Alateya, A., Jha, S. K., Ghozy, S., Kallmes, D. F., & Brinjikji, W. (2024). Current Stroke Solutions Using Artificial Intelligence: A Review of the Literature. *Brain Sciences*, *14*(12), 1182. https://doi.org/10.3390/brainsci14121182

[3] Chan, T. F., & Vese, L. A. (2001). Active contours without edges. *IEEE Transactions on Image Processing*, *10*(2), 266–277. https://doi.org/10.1109/83.902291

[4] Chawla, M., Sharma, S., Sivaswamy, J., & Kishore, L. T. (2009). A method for automatic detection and classification of stroke from brain CT images. *2009 Annual International Conference of the IEEE Engineering in Medicine and Biology Society*, 3581–3584. https://doi.org/10.1109/IEMBS.2009.5335289

[5] Chudasama, D., Patel, T., Joshi, S., & I. Prajapati, G. (2015). Image Segmentation using Morphological Operations. *International Journal of Computer Applications*, *117*(18), 16–19. https://doi.org/10.5120/20654-3197

[6] Elsayed, O., Mahar, K., Kholief, M., & Khater, H. A. (2015). Automatic detection of the pulmonary nodules from CT images. *2015 SAI Intelligent Systems Conference (IntelliSys)*, 742–746. https://doi.org/10.1109/IntelliSys.2015.7361223

[7] Ghazali, K. H., Mansor, M. F., Mustafa, Mohd. M., & Hussain, A. (2007). Feature Extraction Technique using Discrete Wavelet Transform for Image Classification. *2007 5th Student Conference on Research and Development*, 1–4. https://doi.org/10.1109/SCORED.2007.4451366

[8] Goldman, L. W. (2007). Principles of CT and CT Technology. *Journal of Nuclear Medicine Technology*, *35*(3), 115–128. https://doi.org/10.2967/jnmt.107.042978

[9] Hudyma, E., & Terlikowski, G. (2008). Computer-aided detecting of early strokes and its evaluation on the base of CT images. *2008 International Multiconference on Computer Science and Information Technology*, 251–254. https://doi.org/10.1109/IMCSIT.2008.4747247

[10] Jayachitra, S., & Prasanth, A. (2021). Multi-Feature Analysis for Automated Brain Stroke Classification Using Weighted Gaussian Naïve Bayes Classifier. *Journal of Circuits, Systems and Computers*, *30*(10), 2150178. https://doi.org/10.1142/S0218126621501784

[11] Li, L., Wei, M., Liu, B., Atchaneeyasakul, K., Zhou, F., Pan, Z., Kumar, S. A., Zhang, J. Y., Pu, Y., Liebeskind, D. S., & Scalzo, F. (2021). Deep Learning for Hemorrhagic Lesion Detection and Segmentation on Brain CT Images. *IEEE Journal of Biomedical and Health Informatics*, *25*(5), 1646–1659. https://doi.org/10.1109/JBHI.2020.3028243

[12] Lorensen, W. E., & Cline, H. E. (1987). Marching cubes: A high resolution 3D surface construction algorithm. *ACM SIGGRAPH Computer Graphics*, *21*(4), 163–169. https://doi.org/10.1145/37402.37422

[13] Nugroho, P. A., Basuki, D. K., & Sigit, R. (2016). 3D heart image reconstruction and visualization with marching cubes algorithm. *2016 International Conference on Knowledge Creation and Intelligent Computing (KCIC)*, 35–41. https://doi.org/10.1109/KCIC.2016.7883622

[14] Oo, S. Z., & Khaing, A. S. (2014). Brain tumor detection and segmentation using watershed segmentation and morphological operation. *International Journal of Research in Engineering and Technology*, *03*(03), 367–374. https://doi.org/10.15623/ijret.2014.0303068

[15] Orazayeva, A., Tussupov, J., Wójcik, W., Pavlov, S., Abdikerimova, G., & Savytska, L. (2022). Methods for detecting and selecting areas on texture biomedical images of breast cancer. *Informatyka, Automatyka, Pomiary w Gospodarce i Ochronie Środowiska*, *12*(2), 69–72. https://doi.org/10.35784/iapgos.2951

[16] Otsu, N. (1979). A Threshold Selection Method from Gray-Level Histograms. *IEEE Transactions on Systems, Man, and Cybernetics*, *9*(1), 62–66. https://doi.org/10.1109/TSMC.1979.4310076

[17] Ozaltin, O., Coskun, O., Yeniay, O., & Subasi, A. (2022). A Deep Learning Approach for Detecting Stroke from Brain CT Images Using OzNet. *Bioengineering*, *9*(12), 783. https://doi.org/10.3390/bioengineering9120783
[18] Patel, A., & Mehta, K. (2012). 3D Modeling and Rendering of 2D Medical Image. *2012 International Conference on Communication Systems and Network Technologies*, 149–152. https://doi.org/10.1109/CSNT.2012.41
[19] Patel, J. M., & Gamit, N. C. (2016). A review on feature extraction techniques in Content Based Image Retrieval. *2016 International Conference on Wireless Communications, Signal Processing and Networking (WiSPNET)*, 2259–2263. https://doi.org/10.1109/WiSPNET.2016.7566544
[20] Pawar, A. G., & Baraskar, T. N. (2013). Conversion of DICOM Images to Common Standard Image Formats. *International Journal of Emerging Technology and Advanced Engineering*, *3*(2), 627–631.
[21] Prasad, G., Gaddale, V. S., Kamath, R. C., Shekaranaik, V. J., & Pai, S. P. (2024). A Study of Dimensionality Reduction in GLCM Feature-Based Classification of Machined Surface Images. *Arabian Journal for Science and Engineering*, *49*(2), 1531–1553. https://doi.org/10.1007/s13369-023-07854-1
[22] Qari, S., & Thafar, M. A. (2025). Brain Stroke Classification Using CT Scans with Transformer-Based Models and Explainable AI. *Diagnostics*, *15*(19), 2486. https://doi.org/10.3390/diagnostics15192486
[23] Rudie, J. D., Weiss, D. A., Colby, J. B., Rauschecker, A. M., Laguna, B., Braunstein, S., Sugrue, L. P., Hess, C. P., & Villanueva-Meyer, J. E. (2021). Three-dimensional U-Net Convolutional Neural Network for Detection and Segmentation of Intracranial Metastases. *Radiology: Artificial Intelligence*, *3*(3), e200204. https://doi.org/10.1148/ryai.2021200204
[24] Selvakumar, J., Lakshmi, A., & Arivoli, T. (2012). *Brain tumor segmentation and its area calculation in brain MR images using K-mean clustering and Fuzzy C-mean algorithm*. 186–190. https://ieeexplore.ieee.org/document/6215996
[25] Shanthi, A. S., & Karthikeyan, M. (2014). Support Vector Machine for MRI Stroke Classfication. *International Journal on Computer Science and Engineering*, *6*(4), 156–163.
[26] Sreedhar, K. (2012). Enhancement of Images Using Morphological Transformations. *International Journal of Computer Science and Information Technology*, *4*(1), 33–50. https://doi.org/10.5121/ijcsit.2012.4103
[27] Vacek, A., Mair, G., White, P., Bath, P. M., Muir, K. W., Al-Shahi Salman, R., Martin, C., Dye, D., Chappell, F. M., Von Kummer, R., Macleod, M., Sprigg, N., & Wardlaw, J. M. (2024). Evaluating artificial intelligence software for delineating hemorrhage extent on CT brain imaging in stroke. *Journal of Stroke and Cerebrovascular Diseases*, *33*(1), 107512. https://doi.org/10.1016/j.jstrokecerebrovasdis.2023.107512

Dr. Rithu James
e-mail: rithu_james@rajagiritech.edu.in

Rithu James is working as an associate professor in the Department of Electronics and Communication Engineering, Rajagiri School of Engineering and Technology.
Her areas of interest includes signal processing, image processing, state space analysis and biomedical signal processing.

https://orcid.org/0000-0001-5481-2512

Appukuttan Harsha
e-mail: harshaa@rajagiritech.edu.in

Ms. Appukuttan Harsha is working as an assistant professor in the Department of Electronics and Communication Engineering, Rajagiri School of Engineering and Technology.
Research areas are signal processing, medical signal processing and communication engineering.

https://orcid.org/0000-0003-2848-2075

Liza Annie Joseph
e-mail: liza_annie@rajagiritech.edu.in

Ms. Liza Annie Joseph is working as an assistant professor in the Department of Applied Electronics and Instrumentation Engineering in Rajagiri School of Engineering and Technology.
Her areas of interest are instrumentation and biomedical signal processing.

https://orcid.org/0000-0003-1603-4347